6058 *Macromolecules* **2010**, *43*, 6058–6066
DOI: 10.1021/ma101108g

Macromolecules
ARTICLE

Super Toughened Poly(lactic acid) Ternary Blends by Simultaneous Dynamic Vulcanization and Interfacial Compatibilization

Hongzhi Liu, Feng Chen, Bo Liu, Greg Estep, and Jinwen Zhang*

Composite Materials and Engineering Center, Washington State University, Pullman, Washington 99164-1806

Received May 18, 2010; Revised Manuscript Received June 16, 2010

ABSTRACT: In this study, a poly(lactic acid) (PLA) ternary blend system consisting of PLA, an epoxy-containing elastomer, and a zinc ionomer was introduced and studied in detail. Transmission electron microscopy revealed that the "salami"-like phase structure was formed in the ternary blends. While increase in blending temperature had little effects on the tensile properties of the resulting blends, it greatly changed the impact strength. For the blends prepared at 240 °C by extrusion blending, the resulting PLA ternary blends displayed supertoughness with moderate levels of strength and modulus. It was found that the zinc ions catalyzed the cross-linking of epoxy-containing elastomer and also promoted the reactive compatibilization at the interface of PLA and the elastomer. Both blending temperature and elastomer/ionomer ratio were found to play important roles in achieving supertoughness of the blends. The significant increase in notched impact strength was attributed to the effective interfacial compatibilization at elevated blending temperatures.

1. Introduction

Because of its high strength and stiffness, excellent transparency, and biodegradability, poly(lactic acid) (PLA) is a promising alternative to some petroleum-based polymers. Unfortunately, the inherent brittleness of PLA is a major drawback to prevent it from wide applications. Many efforts have been made to improve PLA toughness in the literature,[1] and polymer melt blending is the most economic and practical route. Various biodegradable or nonbiodegradable polymers, such as poly(butylene adipate-*co*-terephthalate),[2,3] polycaprolactone,[4] polyhydroxyalkanoate copolymers (e.g., Nodax),[5,6] poly(butylene succinate),[7] poly(ether)urethane elastomer,[8] hyperbranched polymer (HBP),[9] polyamide elastomer,[10] modified soybean oil,[11] acrylonitrile−butadiene−styrene copolymer (ABS),[12] thermoplastic polyolefin elastomer (TPO),[13] poly(ethylene-*co*-glycidyl methacrylate) (EGMA),[14] polyethylene,[15,16] and glycidyl methacrylate grafted poly(ethylene-*co*-octene) (GMA-*g*-POE),[17] have been used as toughners for PLA. In order to overcome the immiscibility of PLA with impact modifiers used, suitable block or graft copolymers that are either premade or in situ formed during reactive compatibilization were added.[3,6,12,15,16] These PLA blends universally displayed a significant increase in tensile toughness (or ductility) compared to neat PLA. However, most above blends yielded very limited enhancement in impact strength, especially in the notched situation. Recently, Oyama[14] reported supertough PLA/EGMA (80/20, w/w) blends via reactive blending. The injection molded specimens of the blends exhibited notched Charpy impact strengths which were only 2−3 times that of the neat PLA. After annealing at 90 °C for 2.5 h, however, the impact strength of the blend increased to 72 kJ/m^2, ca. 50 times that of the neat PLA. The author deduced from differential scanning calorimetry (DSC) and wide-angle X-ray diffraction (WAXD) results that the crystallization of the PLA matrix played a key role in such significant enhancement. Anderson et al. also reported supertough binary PLA/PE (80/20) blends by using polylactide−polyethylene diblock (i.e., PLA-*b*-PE) copolymers as compatibilizers.[15,16] By varying the structure and amount of the block copolymers and the tacticity nature of the PLA matrix, supertoughness (> ∼530 J/m)[18] under notched Izod impact tests was obtained. Tensile strength and stiffness of the blends suffered a reduction by a factor of 2−3 in all cases relative to the neat PLLA. The magnitude of improvement in impact toughness was believed to be correlated with the improved interfacial adhesion induced by the addition of PLA-*b*-PE copolymers. Like many aliphatic polyesters, however, PLA easily undergoes thermal degradation during molten processing (e.g., via hydrolysis, zipperlike depolymerization, oxidative, random main-chain scission, and transesterification).[19] In turn, the resulting reduction in molecular weight adversely affects the final properties of the materials.[20,21] Since the extent of thermal degradation was closely related to the process condition (both temperature and residence time),[20,21] the importance of minimizing the residence time and processing temperature is usually highlighted during PLA processing.

Dynamic vulcanization refers to a process of selectively vulcanizing an elastomer during its intimate melt mixing with a nonvulcanizing thermoplastic polymer, leading to a two-phase material in which particulate cross-linked elastomer phases are dispersed in a melt-processable plastic matrix.[22] It is an important and versatile route to produce new thermoplastic elastomers. In this study, a novel PLA ternary blend system consisting of PLA, elatomeric ethylene−butyl acrylate−glycidyl methacrylate terpolymer (EBA-GMA), and zinc ionomer of ethylene−methyacrylic acid copolymer (EMAA-Zn) was investigated. It was demonstrated by torque rheological and FT-IR data that dynamic vulcanization between the epoxy-containing elastomer and zinc ionomer occurred within PLA matrix during melt extrusion. Elevated blending temperature (240 °C) not only led to more cross-linking of the elastomeric terpolymer but also triggered reactive compatibilization at the PLA/EBA-GMA interface. Effects of EBA-GMA/EMAA-Zn and blending temperature on

*To whom correspondence should be addressed: Tel (509) 335-8723; Fax (509) 335-5077; e-mail jwzhang@wsu.edu.

 Published on Web 06/30/2010 © 2010 American Chemical Society

Table 1. Characteristics of Materials Used in This Study

polymer (abbreviation)	grade (supplier)	specifications
poly(lactide) (PLA)	PLA2002D (NatureWorks)	MI (210 °C, 2.16 kg) = 5−7 g/10 min
ethylene/*n*-butyl acrylate/glycidyl methacrylate copolymer (EBA-GMA)	Elvaloy PTW (DuPont Co.)	MI (190 °C, 2.16 kg) = 12 g/10 min melting point (DSC) = 72 °C E/BA/GMA = 66.75/28/5.25 (wt %)[23]
ethylene/*n*-butyl acrylate copolymer (EBA)	Lotryl 30BA02 (Arkema Inc.)	MI (190 °C, 2.16 kg) = 1.5−2.5 g/10 min melting point (DSC) = 78 °C BA content = 27−32 wt %
zinc ionomer of ethylene/methacryalic acid copolymer (EMAA-Zn)	Surlyn 9945 (DuPont Co)	MI (190 °C, 2.16 kg) = 4.0 g/10 min melting point (DSC) = 89 °C methacrylic acid content = 15.0 wt % zinc oxide content = 3.70 wt % neutralization = ∼40%[24]
ethylene/methacrylic acid copolymer (EMAA-H)	Nucrel 925 (DuPont Co.)	MI (190 °C, 2.16 kg) = 25 g/10 min melting point (DSC) = 92 °C methacrylic acid content = 15.0 wt %

tensile and impact properties were studied, and supertoughened PLA ternary blends with moderate strength and modulus were successfully achieved by melt-blending at 240 °C and 50 rpm, at which excessive thermal degradation of PLA probably took place.[20] To the best of our knowledge, a similar reactive compatibilizing and toughening route for supertoughened PLA blends via dynamic vulcanization under such elevated blending temperature as 240 °C has not been reported elsewhere.

2. Experimental Section

2.1. Materials and Sample Preparation. The materials used and some specifications are summarized in Table 1. Prior to extrusion, PLA, EMAA-Zn, and EMAA-H pellets were dried for at least 12 h at 80 °C in a convection oven. Melt blending was performed using a corotating twin screw extruder (Leistritz ZSE-18) with a screw diameter of 17.8 mm and an L/D ratio of 40 at a screw speed of 50 rpm. Two barrel temperatures (185 and 240 °C) at kneading zones were chosen to compare the effect of blending temperature. For all blends, the PLA content was fixed at 80 wt % on the basis of total blend weight. Prior to injection molding, the compounds were dried at 80 °C overnight in a convection oven. Specimens for mechanical properties measurement were injection molded (Sumitomo SE50D) at melt temperature of 190 °C and mold temperature of 35 °C. All test specimens were conditioned for 7 days at 23 °C and 50% RH prior to testing and characterization. For comparison, neat PLA was also extruded at 185 and 240 °C, respectively, designated as "PLA-185°C" and "PLA-240°C".

2.2. Mechanical Test. Tensile tests were conducted on a universal testing machine (Instron 4466) following ASTM D638. The crosshead speed was 5.08 mm/min, and the initial strain was measured using a 50.8 mm extensometer. Notched Izod impact tests were performed according to ASTM D256 using a BPI-0-1 Basic Pendulum Impact tester (Dynisco, MA). An average value of five replicated specimens was taken for each composition.

2.3. Electron Microscopy. Cryo-fractured and room-temperature impact-fractured surfaces of specimens were sputter-coated with gold and then examined for morphological structure through a Quanta 200F field emission scanning electron microscope (FE-SEM, FEI Co.) at an accelerated voltage of 15 kV. The substructural morphology of dispersed phases was studied using transmission electron microscopy (TEM, JEOL 1200 EX) at an accelerated voltage of 100 kV. At least 330 particles from four independent TEM images were analyzed to calculate weight-average particle diameter (d_w) using the following equation:

$$d_w = \frac{\sum n_i d_i^2}{\sum n_i d_i} \quad (1)$$

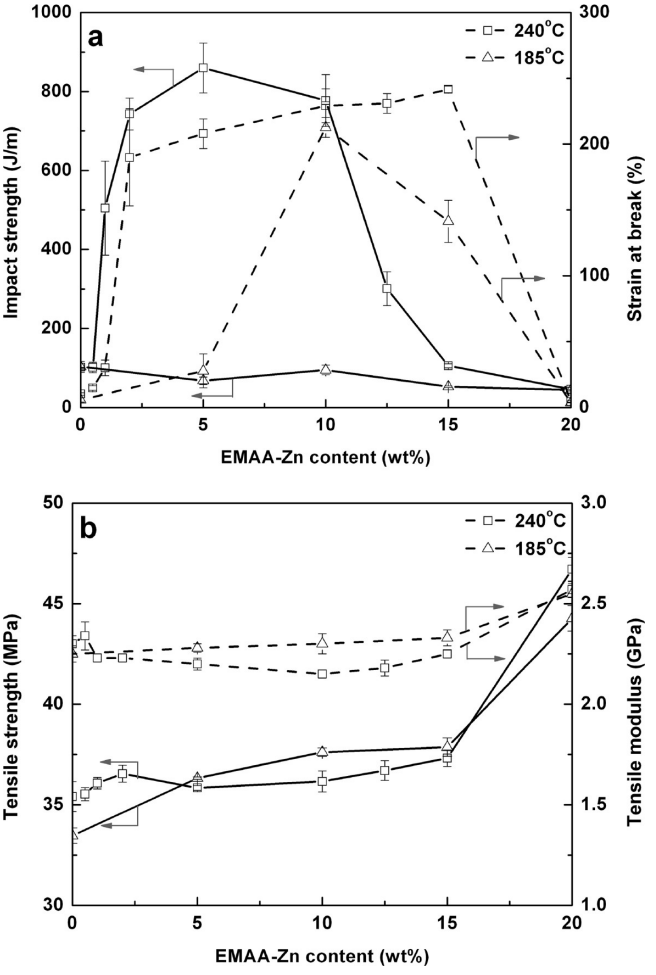

Figure 1. Mechanical properties of PLA/EBA-GMA/EMAA-Zn (80/x/y in weight, $x + y = 20$) blends as functions of weight content of added EMAA-Zn under 240 °C vs 185 °C: (a) impact strength (solid line) and strain at break (%) (dashed line); (b) tensile strength (solid line) and tensile modulus (dashed line).

where n_i is the number of particles having the particle diameter d_i. The particle size polydispersity was represented as the ratio of weight-average particle diameter (d_w) to number-average particle diameter (d_n), i.e., d_w/d_n. Additionally, particles whose sizes were too small to be properly measured at the magnification chosen were neglected.

2.4. Torque Rheology. In order to detect the chemical reactions during compounding, a torque rheometer (Haake Rheomix

Table 2. Mechanical Properties of Binary and Ternary Blends

blend composition	extrusion temperature (°C)	tensile strength (MPa)	tensile modulus (GPa)	strain at break (%)	notched impact strength (J/m)
neat PLA	185	58.2 ± 1.1	3.5 ± 0.03	5.5 ± 1.0	38.0 ± 3.0
	240	61.2 ± 0.4	3.4 ± 0.1	4.5 ± 0.4	24.6 ± 4.7
PLA/EBA-GMA (80/20)	185	33.5 ± 0.4	2.3 ± 0.0	5.7 ± 1.6	102.9 ± 8.7
	240	35.4 ± 0.7	2.3 ± 0.0	10.2 ± 0.8	101.9 ± 13.9
PLA/EMAA-Zn (80/20)	185	44.3 ± 0.6	2.6 ± 0.1	3.7 ± 0.2	43.4 ± 1.9
	240	46.7 ± 0.6	2.6 ± 0.0	4.5 ± 0.9	45.8 ± 4.7
PLA/EBA-GMA/EMAA-Zn (80/10/10)	185	37.6 ± 0.2	2.3 ± 0.1	212.7 ± 7.6	94.5 ± 12.0
	240	36.2 ± 0.5	2.2 ± 0.0	229.1 ± 12.8	777.2 ± 65.8
PLA/EBA-GMA/EMAA-H (80/10/10)	240	35.6 ± 0.5	2.2 ± 0.1	217.2 ± 5.2	97.4 ± 9.9
PLA/EBA/EMAA-Zn (80/10/10)	240	36.5 ± 0.2	2.4 ± 0.1	4.1 ± 0.3	42.5 ± 5.3

600p) was utilized to compound at the same rotation speed and blending temperatures as extrusion processing, i.e., 50 rpm and 185 vs 240 °C. During the entire mixing period, the torque values were recorded as a function of mixing time.

2.5. Analysis of Crystallization. The crystallinity of the PLA matrix phase can influence the mechanical properties of the blends, so thermal analysis was performed using a Mettler Toledo DSC 822e under a nitrogen atmosphere. About 5 mg samples taken from the sample location in injection-molded specimens were heated to 200 °C at a heating rate of 10 °C/min. The crystallinity of PLA (X_c) in the injection specimens was estimated by first heating cycle using the following equation

$$X_c = \frac{\Delta H_m - \Delta H_c}{w_f \Delta H_m^\circ} \times 100\% \quad (5)$$

where ΔH_m and ΔH_c are the enthalpies of melting and cold crystallization during the heating, respectively; ΔH_m° is the enthalpy assuming 100% crystalline PLA homopolymers (93.7 J/g),[25] and w_f is the weight fraction of PLA component in the blend.

Crystallization morphologies were observed using a polarized optical microscope (Olympus BX-51) equipped with a digital image record system. Samples in the form of flat slices with about 20 μm in thickness were cut from injection-molded specimens using a Microtome 860 (America Optical Co.).

2.6. Fourier Transform Infrared Spectroscopy (FT-IR). The spectra were recorded using a Thermo Nicolet Nexus 670 spectrometer (Nicolet). Thin films of as-extruded PLA, EBA-GMA, EMAA-H, and EMAA-Zn samples were prepared by casting from their dilute solutions (chloroform for PLA and EBA-GMA; hot tetrahydrofuran for EMAA-H and EMAA-Zn). For the ternary blends, the slices (~120 μm in thickness) cut from injection-molded specimens were first extracted with chloroform under stirring at ambient temperature for 10 days to thoroughly etch the free PLA and EBA-GMA components. A certain amount of the dried insoluble residues after the extraction was grinded with KBr powder and then compressed into discs for the FT-IR test. All samples were oven-dried under vacuum to eliminate effects of residual solvent and moistures.

2.7. Size-Exclusion Chromatography (SEC). In the case of ternary blends, the solutions left after the extraction in chloroform were filtered, followed by the precipitation in excessive cold methanol. The obtained off-white precipitates were collected via the centrifugation and then dried under vacuum until constant weight for SEC analysis.

The absolute molecular weight (M_n) and molecular weight distribution (i.e., polydispersity index, PDI = M_w/M_n) of neat PLA samples and the above PLA isolates from the ternary blends were determined using an Agilent 1100 system (Agilent 1100 series degasser, isocratic pump and autosampler) equipped with two Phenomenex 10 μm, 300 × 7.8 mm columns [105 Å and MXA], Wyatt DAWN EOS multiangle light scattering (MALS) detector (He−Np 5 mW laser at λ = 632.8 nm), and Agilent 1200 differential refractive index (DRI) detector. Tetrahydrofuran was used as the eluent at a flow rate of 1.0 mL/min. The detectors temperature was 25 °C. The samples were dissolved in chloroform with the concentration of 20 mg/mL and injected by 25 μL.

3. Results and Discussion

3.1. Mechanical Properties. Figure 1 shows effects of mixing temperature and weight ratio of EBA-GMA/EMAA-Zn (total 20 wt % in the blend) on tensile and impact properties of the blends. The impact strength of binary (with only EBA-GMA or EMAA-Zn) blends extruded at 185 °C only exhibited slight improvement (less than 3-fold) with respect to that of neat PLA, as shown in Table 2, and showed little change with temperature increasing to 240 °C. Surprisingly, a remarkable dependence of impact strength on extrusion temperature was found for the ternary blends. The ternary blends prepared at 185 °C displayed similar impact strength to that of binary blends, only showing a slight toughening effect. The ternary blends prepared at 240 °C displayed a tremendous toughening effect except for the one with 0.5 wt % EMAA-Zn. The enhancement in impact strength was more pronounced for the EBA-GMA rich ternary blends. Especially, the ternary blend with 15 wt % EBA-GMA had impact strength of 860 J/m, approximately being 35 times that of the neat PLA prepared at 240 °C. Since such high impact strength was not achievable in either above binary system, these results indicate that there existed a synergistic effect between both modifiers in achieving supertough PLA blends at 240 °C. Likewise, the ternary blends extruded at 240 °C uniformly showed a higher strain at break than those extruded at 185 °C. It is worth mentioning that in this ternary blend system the remarkable enhancement in impact strength was accompanied by high ductility with strain at break in the range of 150−250%. This was evidently different from the results reported by Oyama in the study of PLA/EGMA (80/20, w/w) blends which also displayed the similar supertoughness but substantially lower strain at break (≤35%) after annealing of the modeled samples.[14] In that case, Oyama ascribed the high impact strength obtained to crystallization of the PLA matrix caused by annealing. Because no post-treatment was needed, the ternary blend system in this study for achieving supertoughness was apparently more facile from the industrial point of view. Unlike the impact strength, tensile strength and modulus of the blends were less affected by mixing temperature. Similar to most toughened PLA blends, in this study tensile strength and modulus of the blends suffered a decrease of 34−42% and 31−38%, respectively, with respect to those of the neat PLA samples.

In order to understand the role of EMAA-Zn in the reactive compatibilization of the ternary blends, a non-neutralized ethylene/methacrylic acid copolymer, i.e. EMAA-H, was chosen as an alternative to EMAA-Zn in the above ternary blends. Both polymers were reported to have similar weight content of MAA comonomer (Table 1).

Similarly, to understand the role of EBA-GMA in the reactive compatibilization of the ternary blends, a non-GMA-containing ethylene/*n*-butyl acrylate compolymer, i.e. EBA, was also used to substitute EBA-GMA in the above ternary blends. Table 2 shows the comparison of mechanical properties of various ternary blends. For reference, the mechanical properties of neat PLA and some binary PLA blends are also given in Table 2. When EMAA-H was used in the place of EMAA-Zn, the ternary blend failed to achieve the same level of impact toughness although still yielded remarkable tensile strain at break. Like the case for the PLA/EBA-GMA and PLA/EMAA-Zn binary blends, this mild improvement in impact strength was likely attributed to the insufficient interfacial adhesion, as revealed in the later SEM analysis. Since Zn salts are able to catalyze transesterification between polyesters,[26,27] in these studies the interfacial compatibilization may stem from possible transesterification between PLA and BA ester groups in EBA-GMA catalyzed by the Zn cation of the ionomer. The role of epoxy functional groups (GMA) in the reactive compatibilization could be well identified by replacing EBA-GMA by EBA in the ternary blends, and the latter has similar BA content to the former, as shown in Table 1. As a result (Table 2), this substitution resulted in the loss of both impact strength and tensile strain at break of the ternary blends. These results demonstrate that it was not the transesterification between ester groups of both PLA and EBA-GMA but the compatibilization reactions of epoxy groups catalyzed by Zn ions that mainly contributed to the above supertoughness in ternary blends prepared at 240 °C. In the case of tensile strength and modulus, these ternary blends differed slightly otherwise, implying that the strength and modulus of such ternary blends were mainly determined by the content of major PLA phase.

Table 3. SEC Analysis of PLA Component in Both Ternary Blends and Neat PLAs

sample	M_n (g mol^{-1})	PDI
unprocessed PLA	120 500	1.23
PLA-240 °C	101 700	1.24
PLA-185 °C	108 600	1.25
PLA/EBA-GMA/EMAA-Zn (80/10/10), 240 °C	91 300	1.25
PLA/EBA-GMA/EMAA-Zn (80/10/10), 185 °C	106 700	1.24

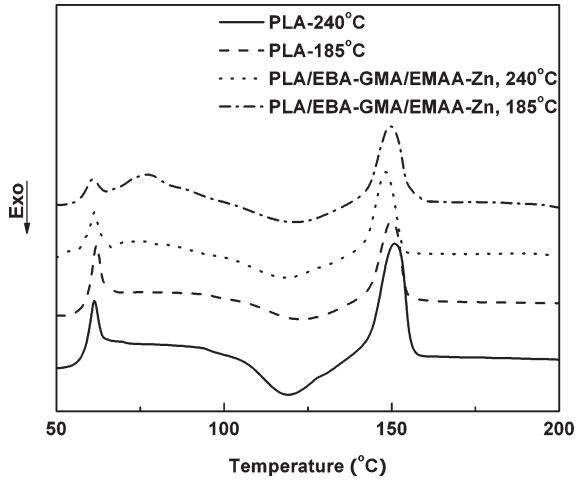

Figure 2. DSC thermogramic curves of neat PLAs and PLA/EBA-GMA/EMAA-Zn (80/10/10) ternary blends extruded at 185 and 240 °C during first heating.

PLA is susceptible to thermal or hydrolytic degradation in melt processing, resulting in a reduction of molecular weight that may affects mechanical properties of the final products (e.g., impact strength).[20,21,28] Table 3 shows the effects of processing temperature on the number-average molecular weight (M_n) and molecular weight distribution (PDI) of PLA. Compared to the unprocessed PLA, neat PLA and PLA in the blends all displayed reductions in molecular weight, depending on extrusion temperatures. Neat PLA processed at 185 and 240 °C displayed an approximate 10% and 16% reduction in M_n, respectively. On the other hand, PLA in the ternary blends underwent somewhat larger reductions in M_n, showing ca. 11 and 24% decreases for the blends extruded at 185 and 240 °C, respectively. Some studied have demonstrated that tensile and impact properties of PLA decrease as the molecular weight of PLA is reduced under different processing conditions.[20,21,28] However, such changes in properties with molecular weight are gradual rather than drastic. Therefore, the ~14% reduction in PLA molecular weight for the ternary blend extruded at 240 °C with respect to that extruded at 185 °C might at most have a very limited influence on the drastically improved impact strength.

Crystallization Analysis. Oyama studied the effects of annealing of PLA/EGMA blends on mechanical properties and concluded that the crystallization of the PLA matrix played a significant role in toughening.[14] For the block copolymer compatibilized PLA/PE blends, however, Anderson and Hillmyer found that the impact strength was not sensitive to the variation of crystallinity within the relatively low level (0 to ca. 8%).[15] In order to clarify whether PLA crystallization had any influence on toughening in our blend system, the crystallization and melting behaviors of the PLA component in the blends were examined. Because it is the crystalline state of PLA in the molded samples which could influence mechanical properties of the blends, only the DSC data from the first heat scan are presented. Figure 2 shows the DSC thermograms of PLA and PLA ternary blends prepared at 185 and 240 °C, respectively. A summary of the DSC results is given in Table 4. Neat PLA and PLA blends exhibited very similar thermograms, all showing cold crystallization of PLA and subsequent melting of PLA crystals. The endothermic peak close T_g was attributed to the enthalpy relaxation effects reflecting the thermal history of the samples.[29] The difference in cold crystallization temperature (T_{cc}) and melting temperature (T_m) between neat PLA and PLA in the blends is not significant and was less influenced by extrusion temperature. Furthermore, the crystallinity of PLA in the ternary blend extruded at 185 °C was slightly higher than that of the PLA in the blend extruded at 240 °C,

Table 4. DSC Results of PLA and PLA/EBA-GMA/EMAA-Zn Blends Extruded

	first heating		
samples	T_m (°C)	T_{cc} (°C)[a]	X_c (%)[b]
PLA-240 °C	150.9	118.8	0.2
PLA-185 °C	150.0	122.5	0.4
PLA/EBA-GMA/EMAA-Zn (80/10/10), 240 °C	148.2	118.1	1.0
PLA/EBA-GMA/EMAA-Zn (80/10/10), 185 °C	149.7	120.8	4.1

[a] T_{cc}: cold crystallization peak temperature. [b] Degree of crystallinity of PLA (X_c) was determined from the first heating curves.

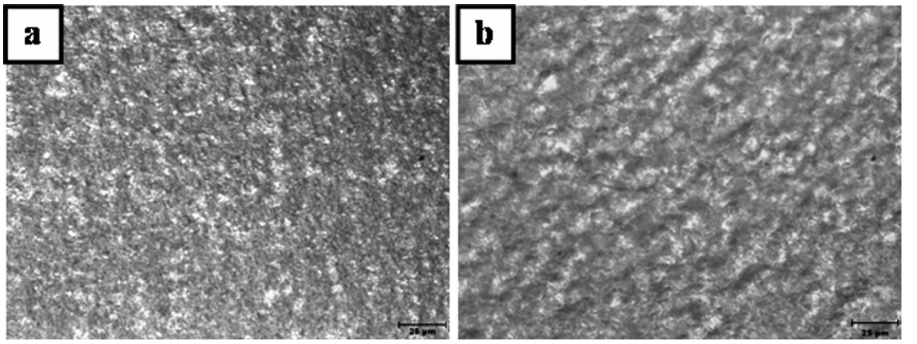

Figure 3. POM micrographs of PLA/EBA-GMA/EMAA-Zn (80/10/10) blends extruded at 240 °C (a) and 185 °C (b). Scale bar: 25 μm.

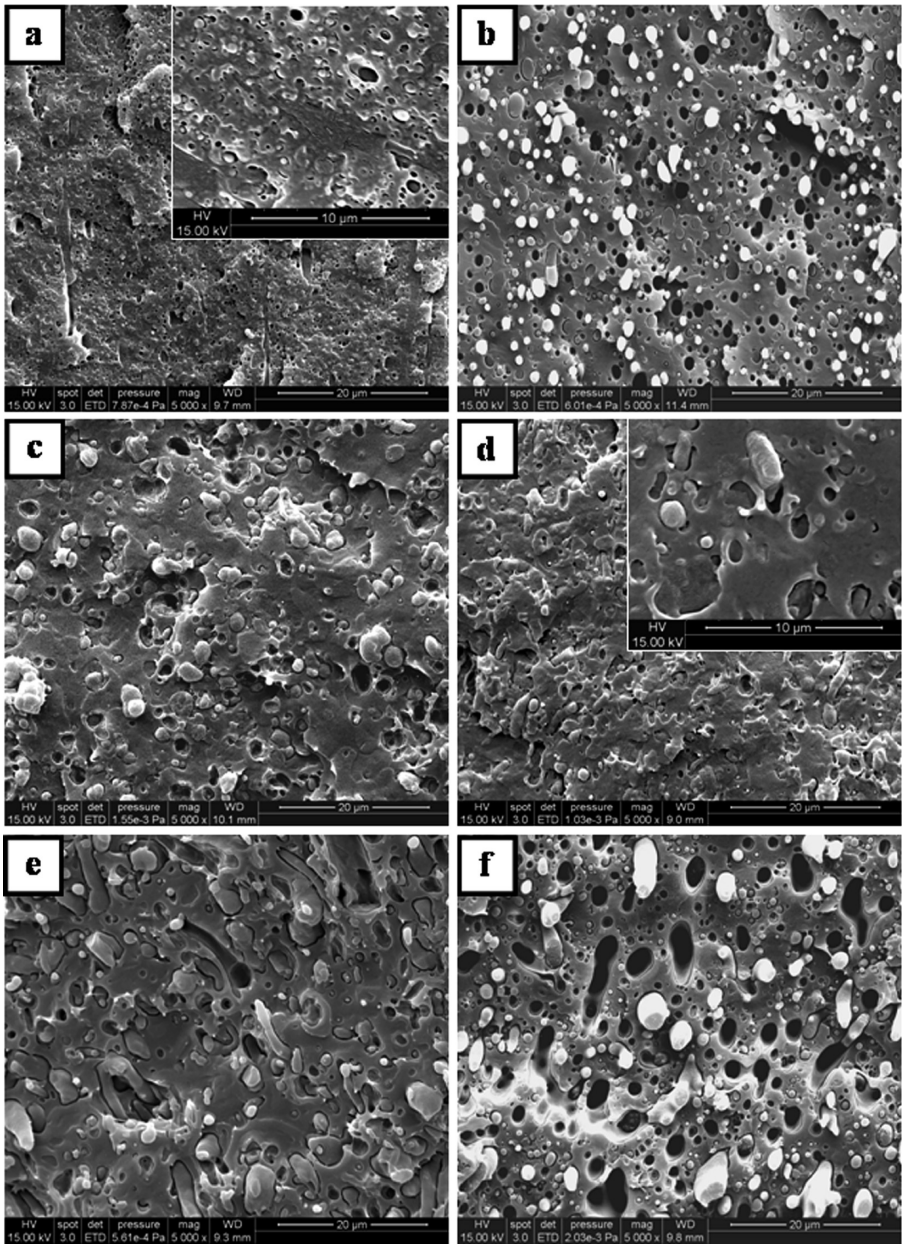

Figure 4. Cryo-fractured SEM images of binary and ternary blends extruded at 50 rpm: (a) PLA/EBA-GMA (80/20), 240 °C (inset: higher magnification); (b) PLA/EMAA-Zn (80/20), 240 °C; (c) PLA/EBA-GMA/EMAA-Zn (80/10/10), 185 °C; (d) PLA/EBA-GMA/EMAA-Zn (80/10/10), 240 °C (inset: higher magnification); (e) PLA/EBA-GMA/EMAA-H (80/10/10), 240 °C; (f) PLA/EBA/EMAA-Zn (80/10/10), 240 °C.

but both at the same low level (< 5%). Figure 3 shows the crystallization morphologies of molded ternary blends. The POM samples were prepared by slicing both PLA/EBA-GMA/EMAA-Zn (80/10/10) blends extruded at 240 and 185 °C, respectively. On the basis of the above results, therefore, the enhanced crystallization of PLA matrix does

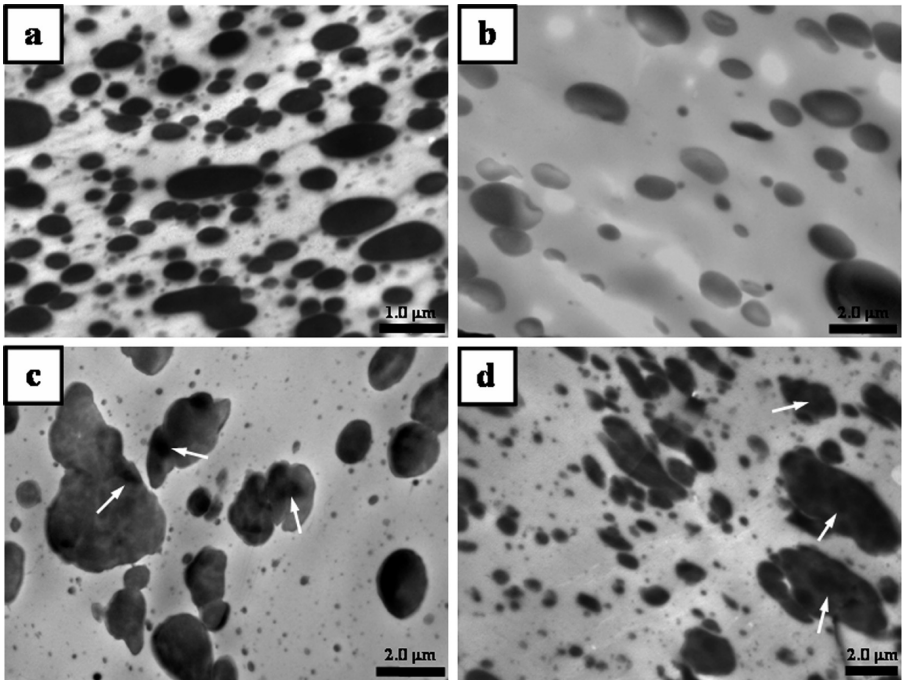

Figure 5. TEM images of binary and ternary blends extruded at 50 rpm: (a) PLA/EBA-GMA (80/20), 240 °C; (b) PLA/EMAA-Zn (80/20), 240 °C; (c) PLA/EBA-GMA/EMAA-Zn (80/10/10), 185 °C; (d) PLA/EBA-GMA/EMAA-Zn (80/10/10), 240 °C.

not appear to be a contributing factor in resulting in the significant dependence of impact toughness on processing temperature.

Morphology. Since mechanical properties of multiphase polymer blends depend largely on the resulting morphologies during melt-blending, both SEM and TEM were employed to identify the phase structure of the above ternary blends. Figure 4 shows cryo-fracture surface SEM micrographs of various PLA-based ternary blends. PLA/EBA-GMA binary blend showed much finer phase structure (Figure 4a) than the PLA/EMAA-Zn binary one (Figure 4b). This result might be attributed to lower interfacial tension or melt viscosity (based on MI values) in the former than in the latter. However, many smooth holes left at both cryo-fractured and impact-fractured (not shown) surfaces of the samples were indicative of still insufficient interfacial adhesions for both binary blends. The ternary PLA/EBA-GMA/EMAA-Zn (80/10/10) blend compounded at 185 °C also exhibited extensive debonding at interfaces (Figure 4c). In contrast, the ternary blend compounded at 240 °C showed much improved wetting of the dispersed phase by the matrix (Figure 4d). Similar to Figure 4b, clear debonding was also seen when either EMAA-H or EBA was utilized (Figure 4e,f). The PLA/EBA-GMA/EMAA-H (80/10/10) blend exhibited more dispersed domains with irregular shape. Thus, the SEM observation was well consistent with their results of mechanical properties. On the basis of the above results, the better wetting of the dispersed phase in the ternary PLA/EBA-GMA/EMAA-Zn blend prepared at 240 °C probably resulted from the increased interfacial reactions between PLA and EBA-GMA under the catalysis of Zn ions at the elevated temperature, as suggested in the FTIR spectra section.

TEM micrographs in Figure 5 further illustrate the phase structures of PLA binary and ternary blends. As shown in Figures 5a,b, both of the binary PLA/EBA-GMA and PLA/EMAA-Zn blends exhibited the common droplet-in-matrix structure, but the former achieved finer dispersed particles (d_w = 0.30 μm) than the latter (d_w = 1.08 μm). This result was consistent with the SEM observation. However, TEM micrographs of both ternary blends (Figure 5c,d) displayed "salami"-like substructure. Although it was hard to clearly distinguish the EBA-GMA domains from the EMAA-Zn ones, the dark inner inclusions were believed to be the EMAA-Zn phase resided in the gray EBA-GMA dispersed phase domains based on the above inference that EBA-GMA has lower interfacial tension with PLA than EMAA-Zn. Both ternary blends exhibited similar weight-average particle sizes (d_w = 0.82 μm for 240 °C versus d_w = 1.01 μm for 185 °C). If the d_w values of the above blends were correlated with their impact strengths, the finest dispersed particle size (Figure 5a) did not mean the highest impact toughness (Figure 1a). Presumably, there was an optimum rubber size at which the blends achieved the maximum impact toughness in our blend system. This might be understood by the fact that if rubber particles were very small, internal cavitations of rubber particles[30−34] or crazes[35] would not be easily initiated. Therefore, the localized matrix yielding needed for effective high impact energy absorption was not promoted. Likewise, the optimum particle size was also reported to exist in some other rubber-toughened blend systems, like nylons,[36−40] poly(methyl methacrylate) (PMMA),[18,41−43] poly(vinyl chloride) (PVC),[44] poly(styrene-*co*-acrylonitrile) (SAN),[45] and polystyrene (PS).[45,46] On the other hand, the ternary blend extruded at 240 °C showed a smaller polydispersity (d_w/d_n) value than the blend extruded at 185 °C, namely 1.96 for 240 °C versus 2.98 for 185 °C. The possible effect of particle size polydispersity on toughening in our blend system is under investigation, and further results will be presented in future work.

Reaction Mechanism. Figure 6 shows the torque change with time during polymer melting or blending performed in a Haake torque rheometer. In Figure 6a, the toque of each individual polymer initially displayed a sharp and strong peak which was attributed to the melting of the pellets and then became very flat, suggesting they are quite thermally stable at the processing conditions. For the mixing of EBA/EMAA-Zn (50/50, w/w) binary blend (Figure 6b), no perceptible increase in toque value was noted after the pellets

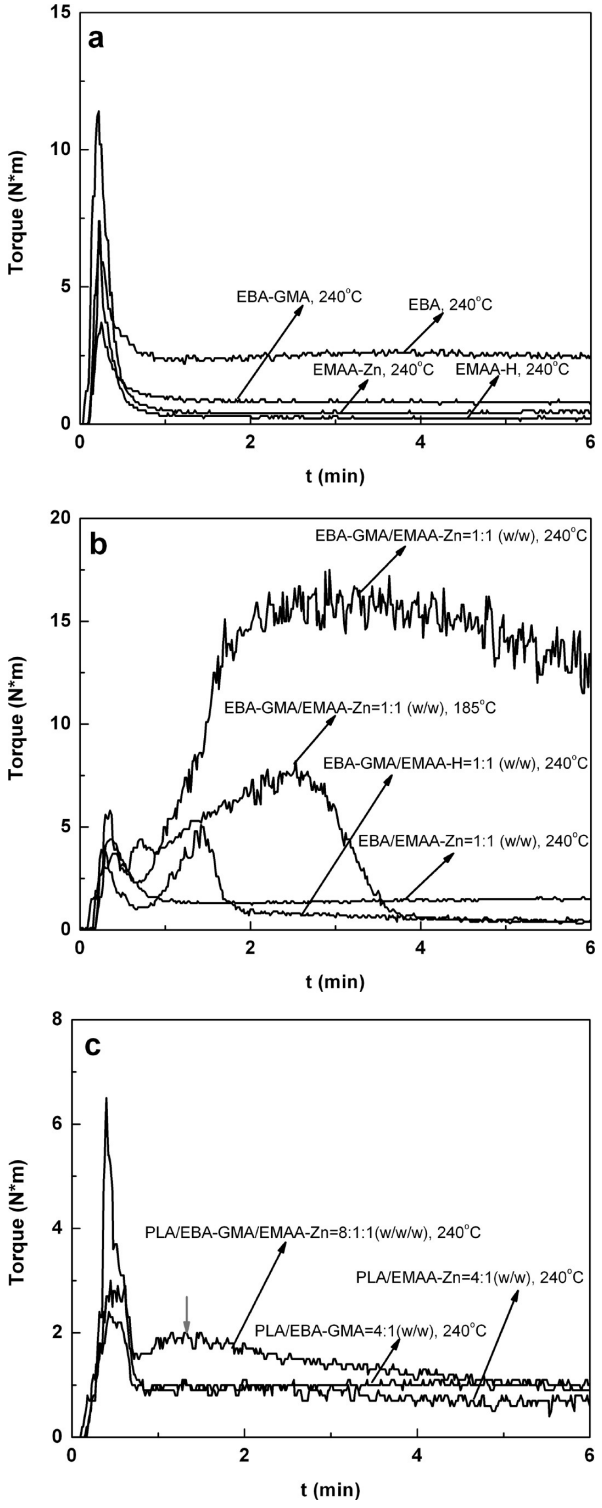

Figure 6. Torque vs time for the melting of individual polymer or mixing of binary blends and ternary blends.

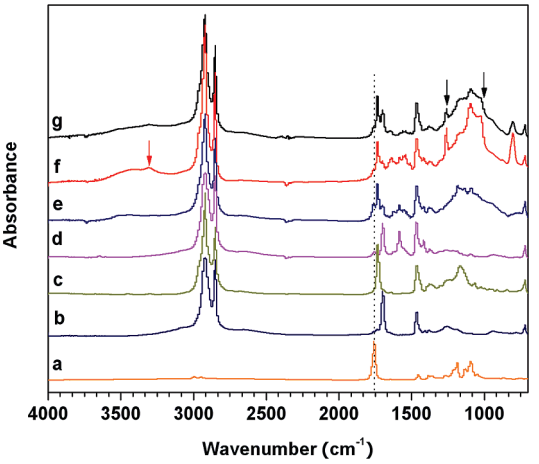

Figure 7. FTIR absorption spectra of individual polymers and ternary PLA blends: (a) neat PLA; (b) neat EMAA-H; (c) neat EBA-GMA; (d) neat EMAA-Zn; (e) chloroform-extracted PLA/EBA-GMA/EMAA-Zn (80/10/10) blend extruded at 240 °C; (f) chloroform-extracted PLA/EBA-GMA/EMAA-Zn (80/10/10) blend extruded at 185 °C; (g) chloroform-extracted PLA/EBA-GMA/EMAA-H (80/10/10) blend extruded at 240 °C.

were fully melted, indicating that no reactions occurred when the EBA rubber does not contain epoxide groups. For the mixing of EBA-GMA/EMAA-H (50/50, w/w) blend, a moderate increment in torque was observed, suggesting the occurrence of chemical reactions between GMA and the carboxylic acid groups of MAA. When EMAA-H in the above mixing was replaced by EMAA-Zn which contained both carboxylic acid groups and Zn ions, a substantially higher torque value was noted. Particularly, more remarkable and rapid increase in torque was noted for mixing at 240 °C than at 185 °C. Within ca. 2−3 min, the maximum torque value was attained. Evidently, the blending at 240 °C would result in higher extent of cross-link reactions. The cross-linking reactions were also evidenced during the mixing of the ternary PLA/EBA-GMA/EMAA-Zn (80/10/10, w/w) blend at 240 °C, as indicated in Figure 6c. In contrast, the mixing of PLA binary blends with either polymer did not suggest the occurrence of cross-linking reactions. These results confirmed that elevated blending temperature further accelerated the Zn^{2+}-catalyzed cross-linking reactions of EBA-GMA.

In order to gain insight into possible structural changes induced by the reactive compatibilization, Figure 7 shows FT-IR spectra of the individual polymers and blends recorded in the range of 700−4000 cm^{-1}. The stretch vibration of ester carbonyl in the PLA backbone was seen at 1759 cm^{-1}, while the vibration of ester carbonyl group of EBA-GMA was located at 1735 cm^{-1}. EMAA-Zn exhibited a weak shoulder peak at 1757 cm^{-1} attributed to the free carboxylic acid groups and a strong absorption at 1698 cm^{-1} due to the carboxylic acid dimer (i.e., hydrogen-bonded COOH groups).[47] In the case of EMAA-H, the large majority of the carboxylic acid (COOH) groups existed as intermolecular dimers, which have a characteristic infrared absorption at 1698 cm^{-1}, and the corresponding O−H stretching frequency for dimer was seen as a broad band at about 3000 cm^{-1} buried beneath the strong, sharp C−H stretching modes.[48]

For the three ternary blends, after removal of both PLA and EBA-GMA phases by chloroform extraction, a strong peak at 1735 cm^{-1} associated with the carbonyl vibration of EBA-GMA still remained, in addition to a shoulder peak at 1698 cm^{-1} attributed to the hydrogen-bonded COOH groups on the EMAA-Zn backbone. Again, this result confirmed the occurrence of curing reactions between EBA-GMA and EMAA-Zn under these conditions. A shoulder peak at 1760 cm^{-1} resulting from the ester carbonyl groups of PLA was also noted for both extracted ternary blends, but this peak appeared stronger in intensity for the PLA/EBA-GMA/EMAA-Zn blend extruded at 240 °C. This result also suggests that more PLA molecules were involved in the coupling reactions at 240 °C. In addition, the other ternary

Scheme 1. Proposed Reactions during Reactive Blending Process, Together with Schematic Phase Morphologies of the PLA/EBA-GMA/EMAA-Zn Ternary Blends Prepared at 185 and 240 °C, Respectively[a]

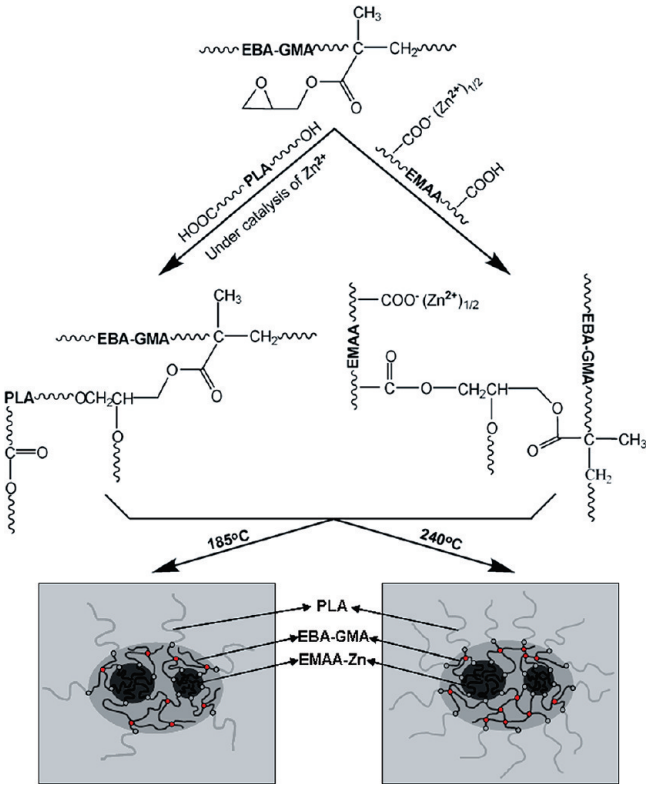

[a] Note: more PLA molecules were grafted at interfaces, and higher cross-linking degree inside EBA-GMA domains resulted for the ternary blend prepared at 240 °C.

blend samples still exhibited the absorption at 1261 and 1017 cm^{-1}, both of which were assigned to the ring vibration of unreacted epoxy groups in EBA-GMA.[49,50] Instead, this characteristic absorption almost disappeared in the spectra of the PLA/EBA-GMA/EMAA-Zn blend extruded at 240 °C due to more consumption of epoxy groups. Another noticeable feature for the ternary blends lied in the stretching vibration of hydroxyl groups in the range of 3100−3600 cm^{-1}. It should be mentioned that the hydroxyl groups resulting from ring-opening of epoxy groups also contributed to the absorption in this region. A relatively weaker overall intensity was visible for the PLA/EBA-GMA/EMAA-Zn sample extruded at 240 °C with respect to the other ternary blends. This could be due to the difference in the degree of cross-linking reaction of epoxy groups between these ternary blends. In the former case, more hydroxyl groups (including hydroxyl groups resulting from the ring-opening of epoxy groups) were consumed via either etherification or further esterification.[51] The stretching vibration of hydroxyl groups in the PLA/EBA-GMA/EMAA-Zn sample extruded at 185 °C evidently split into a bimodal peak (ca. 3500 and 3300 cm^{-1}), which were attributed to the free hydroxyl groups and hydrogen-bonded ones, respectively.[52]

It is known that epoxy can react with both carboxyl and hydroxyl groups to form ester and ether linkages under suitable conditions, respectively, while the reaction with carboxyl group has higher reactivity than the reaction with hydroxyl group.[51] The hydroxyl groups resulted from ring-opening of an epoxy may also participate in curing through reacting with another epoxy and so on, ultimately leading to the formation of cross-linking structure. The rubber curing reactions could be quite complicated, depending on the stoichiometric ratio of the epoxy/carboxyl, catalyst used and concentration, and curing conditions. Lewis acid (e.g., zinc salts) is known to catalyze the curing of epoxy resins.[51] Since NatureWork PLA is synthesized by ring-opening polymerization of lactide using catalyst such as tin(II) octoate, the PLA is mainly terminated with end hydroxyl groups.[53] Therefore, on the basis of the above results, Scheme 1 is proposed to explain the remarkable dependence of impact strength on blending temperature. At 185 °C, moderate curing reactions took place between the carboxyl groups of EMAA-Zn and epoxy groups of EBA-GMA under the catalysis of Zn^{2+} ions, but the compatiblization reactions between the epoxy of EBA-GMA and hydroxyl groups of PLA were not significant. Hence, like many other soft polymer toughened PLA blends, the resulting ternary blend displayed high ductility but only limited improvement in impact strength. At 240 °C, not only was the degree of curing of the EBA-GMA rubber greatly increased but also the compatibilization reactions between the rubber and PLA phases were significant enhanced. Therefore, the resulting interface was able to stabilize premature crack propagation at the early stage of impact test having a high-strain rate before massive matrix shear yielding took place.[42,54,55]

4. Conclusions

Supertoughened PLA ternary blends with moderate strength and stiffness were successfully prepared by melt-blending of PLA with EBA-GMA and EMAA-Zn at 240 °C. TEM revealed a domain-in-domain morphology of the ternary blends. The EMAA-Zn domains were occluded inside the EBA-GMA particles which were homogeneously dispersed in the PLA matrix. Torque analysis during mixing demonstrated that the carboxyl groups in the EMAA-Zn ionomer was able to trigger cross-linking reactions of the epoxy groups in the EBA-GMA phase, and the Zn ions in the ionomer further catalyzed the reactions. DSC and POM results indicated that increasing blending temperature had little effects of on degree of crystallinity and crystallization morphologies of the PLA matrix in the ternary blends. FT-IR study suggests that more PLA was grafted onto EBA-GMA when blending temperature was at 240 °C than at 185 °C, and accordingly SEM micrographs also displayed better wetting of the dispersed phase by the PLA matrix at higher blending temperature. The effective interfacial compatibilization achieved at elevated blending temperatures was mainly responsible for the significant increase in notched impact strength.

Acknowledgment. The authors are grateful for the financial support from the National Research Initiative of the USDA Cooperative State Research, Education and Extension Service, Grant No. 2007-35504-17818. The authors also thank Dr. Sassan Hojabr and Adam G. Lawler at DuPont Co. for kindly providing the materials.

References and Notes

(1) Anderson, K. S.; Shreck, K. M.; Hillmyer, A. M. *Polym. Rev.* **2008**, *48*, 85–108.
(2) Jiang, L.; Wolcott, M. P.; Zhang, J. *Biomacromolecules* **2006**, *7*, 199–207.
(3) Zhang, N.; Wang, Q.; Ren, J.; Wang, L. *J. Mater. Sci.* **2009**, *44*, 250–256.
(4) Semba, T.; Kitagawa, K.; Ishiaku, U. S.; Hamada, H. *J. Appl. Polym. Sci.* **2006**, *101*, 1816–1825.
(5) Noda, I.; Satkowski, M. M.; Dowrey, A. E.; Marcott, C. *Macromol. Biosci.* **2004**, *4*, 269–275.
(6) Schreck, K. M.; Hillmyer, M. A. *J. Biotechnol.* **2007**, *132*, 287–295.
(7) Wang, R.; Wang, S.; Zhang, Y.; Wan, C.; Ma, P. *Polym. Eng. Sci.* **2009**, *49*, 26–33.
(8) Li, Y.; Shimizu, H. *Macromol. Biosci.* **2007**, *7*, 921–928.

(9) Bhardwaj, R.; Mohanty, A. K. *Biomacromolecules* **2007**, *8*, 2476–2484.
(10) Zhang, W.; Chen, L.; Zhang, Y. *Polymer* **2009**, *50*, 1311–1315.
(11) Robertson, M. L.; Chang, K.; Gramlich, W. M.; Hillmyer, M. A. *Macromolecules* **2010**, *43*, 1807–1814.
(12) Li, Y.; Shimizu, H. *Eur. Polym. J.* **2009**, *45*, 738–746.
(13) Ho, C.-H.; Wang, C.-H.; Lin, C.-I.; Lee, Y.-D. *Polymer* **2008**, *49*, 3902–3910.
(14) Oyama, H. T. *Polymer* **2009**, *50*, 747–751.
(15) Anderson, K. S.; Lim, S. H.; Hillmyer, M. A. *J. Appl. Polym. Sci.* **2003**, *89*, 3757–3768.
(16) Anderson, K. S.; Hillmyer, M. A. *Polymer* **2004**, *45*, 8809–8823.
(17) Su, Z.; Li, Q.; Liu, Y.; Hu, G.-H.; Wu, C. *Eur. Polym. J.* **2009**, *45*, 2428–2433.
(18) Wu, S. *Polym. Eng. Sci.* **1990**, *30*, 753–761.
(19) Sodergard, A.; Stold, M. *Prog. Polym. Sci.* **2002**, *27*, 1123–1163.
(20) Taubner, V.; Shishoo, R. *J. Appl. Polym. Sci.* **2001**, *79*, 2128–2135.
(21) Zenkiewicz, M.; Richert, J.; Rytlewski, P.; Moraczewski, K.; Stepczynska, M.; Karasiewicz, T. *Polym. Test.* **2009**, *28*, 412–418.
(22) Coran, A. Y.; Patel, R. P. In *Thermoplastic Elastomers*, 3rd ed.; Holden, G., Kricheldorf, H. R., Quirk, R. P., Eds.; Hanser Publishers: Munich, 2004; Chapter 7, pp 143−181.
(23) Kaci, M.; Cimmino, S.; Silvestre, C.; Duraccio, D.; Benhamida, A.; Zaidi, L. *Macromol. Mater. Eng.* **2006**, *291*, 869–876.
(24) Shah, R. K.; Paul, D. R. *Macromolecules* **2006**, *39*, 3327–3336.
(25) Garlotta, D. *J. Polym. Environ.* **2001**, *9*, 60–84.
(26) Coltelli, M.-B.; Bianchi, S.; Aglietto, M. *Polymer* **2007**, *48*, 1276–1286.
(27) Coltelli, M.-B.; Bianchi, S.; Aglietto, M. *Polymer* **2007**, *48*, 1276–1286.
(28) Perego, G.; Cella, G. D.; Bastioli, C. *J. Appl. Polym. Sci.* **1996**, *59*, 37–43.
(29) Celli, A.; Scandola, M. *Polymer* **1992**, *33*, 2699–2703.
(30) Lazzeri, A.; Bucknall, C. B. *J. Mater. Sci.* **1993**, *28*, 6799–6808.
(31) Dijkstra, K.; Van der Wal, A.; Gaymans, R. J. *J. Mater. Sci.* **1994**, *29*, 3489–3496.
(32) Dompas, D.; Groeninckx, G. *Polymer* **1994**, *35*, 4743–4749.
(33) Dompas, D.; Groeninckx, G.; Isogawa, M.; Hasegawa, T.; Kadokura, M. *Polymer* **1994**, *35*, 4750–4759.
(34) Dompas, D.; Groeninckx, G.; Isogawa, M.; Hasegawa, T.; Kadokura, M. *Polymer* **1994**, *35*, 4760–4765.
(35) Donald, A. M.; Kramer, E. J. *J. Appl. Polym. Sci.* **1982**, *27*, 3729–3741.
(36) Oshinski, A. J.; Keskkula, H.; Paul, D. R. *Polymer* **1992**, *33*, 268–283.
(37) Oshinski, A. J.; Keskkula, H.; Paul, D. R. *Polymer* **1992**, *33*, 284–293.
(38) Oshinski, A. J.; Keskkula, H.; Paul, D. R. *J. Appl. Polym. Sci.* **1996**, *61*, 623–640.
(39) Oshinski, A. J.; Keskkula, H.; Paul, D. R. *Polymer* **1996**, *37*, 4909–4918.
(40) Huang, J. J.; Keskkula, H.; Paul, D. R. *Polymer* **2006**, *47*, 639–651.
(41) Wrotecki, C.; Heim, P.; Gaillard, P. *Polym. Eng. Sci.* **1991**, *31*, 213–217.
(42) Cho, K.; Yang, J. H.; Park, C. E. *Polymer* **1997**, *389*, 5161–5169.
(43) Cho, K.; Yang, J. H.; Park, C. E. *Polymer* **1998**, *39*, 3073–3081.
(44) Takaki, A.; Yasui, H.; Narisawa, I. *Polym. Eng. Sci.* **1997**, *37*, 105–119.
(45) Cigna, G.; Lomellini, P.; Merlotti, M. *J. Appl. Polym. Sci.* **1989**, *37*, 1527–1540.
(46) Donald, A. M.; Kramer, E. *J. Mater. Sci.* **1982**, *17*, 2351–2358.
(47) Coleman, M. M.; Lee, J. Y.; Painter, P. C. *Macromolecules* **1990**, *23*, 2339–2345.
(48) Lee, J. Y.; Painter, P. C.; Coleman, M. M. *Macromolecules* **1988**, *21*, 346–354.
(49) Wang, F.; Xiao, J.; Wang, J.-W.; Li, S. Q. *J. Appl. Polym. Sci.* **2008**, *107*, 223–227.
(50) Do, H.-S.; Park, J.-H.; Kim, H.-J. *J. Appl. Polym. Sci.* **2009**, *111*, 1172–1176.
(51) Mika, T. F. In *Epoxy Resins: Chemistry and Technology*; May, C. A., Tanaka, Y., Eds.; Marcel Dekker: New York, 1973.
(52) Moskala, E. J.; Howe, S. E.; Painter, P. C.; Coleman, M. M. *Macromolecules* **1984**, *17*, 1671–1678.
(53) Kowalski, A.; Duda, A.; Penczek, S. *Macromolecules* **2000**, *33*, 7359–7370.
(54) Kim, G. M.; Michler, G. H. *Polymer* **1998**, *39*, 5689–5697.
(55) Kim, G. M.; Michler, G. H. *Polymer* **1998**, *39*, 5699–5703.